nature cell biology

Growth factor-induced MAPK network topology shapes Erk response determining PC-12 cell fate

Silvia D. M. Santos[1], Peter J. Verveer[1,2] and Philippe I. H. Bastiaens[1,2,3]

The mitogen-activated protein kinase (MAPK) network is a conserved signalling module that regulates cell fate by transducing a myriad of growth-factor signals[1]. The ability of this network to coordinate and process a variety of inputs from different growth-factor receptors into specific biological responses is, however, still not understood. We investigated how the MAPK network brings about signal specificity in PC-12 cells, a model for neuronal differentiation[2]. Reverse engineering by modular-response analysis[3] uncovered topological differences in the MAPK core network dependent on whether cells were activated with epidermal or neuronal growth factor (EGF or NGF). On EGF stimulation, the network exhibited negative feedback only, whereas a positive feedback was apparent on NGF stimulation. The latter allows for bi-stable Erk activation dynamics, which were indeed observed. By rewiring these regulatory feedbacks, we were able to reverse the specific cell responses to EGF and NGF. These results show that growth factor context determines the topology of the MAPK signalling network and that the resulting dynamics govern cell fate.

Rat adrenal pheochromocytoma (PC-12) cells have been used as a model system to address how specific functionality arises from the operation of the MAPK signalling cascade[4]. Here, the MAPK pathway involving the proteins Raf, Mek and Erk is activated through the receptor tyrosine kinases TrkA and epidermal growth factor receptor (EGFR) by two different stimuli, NGF and EGF. The ensuing signalling through the MAPK triad gives rise to opposite cell fates, differentiation and proliferation, respectively. The distinct dynamics of Erk activation are believed to be the underlying cause for the difference in cellular response[4]. On NGF stimulation, Erk showed a sustained activation, whereas EGF induced a transient response (Fig. 1a and see Supplementary Information, Fig. S1a). A model for the molecular interpretation of Erk signal strength and duration by immediate early gene (IEG) products was proposed[5]: IEGs are stabilized by Erk-catalysed phosphorylation only when Erk exhibits sustained activity, thereby resulting in differential gene expression dependent on Erk signal duration. Thus, the remaining question is how the difference in Erk dynamics originates from upstream processes. Several mechanisms have been proposed including differences in receptor downregulation[6,7] and distinct kinetics of small GTPase regulators[8]. However, we envision that Erk activation dynamics are ultimately controlled by the configuration of the network in which it is embedded, where the connections within the MAPK signalling module can adopt different configurations depending on the stimulation context (EGF versus NGF). This implies that the manifestation of different topological features is what determines distinct Erk activation dynamics, and thereby cell fate.

Modular response analysis (MRA), a sensitivity analysis developed by Kholodenko *et al.*[3], was applied to determine the MAPK network architecture in the context of NGF and EGF stimulation (Fig. 1b). This approach is based on experimentally measured network responses, at steady-state conditions, to successive small perturbations (Fig. 1c). The topology of the network cannot be directly derived from the measured global response coefficients (that is, change in activity of each module before and after perturbation), because these reflect the propagation of each perturbation throughout the network. However, a map of network connections can be generated by computing local response coefficients (Fig. 1b), which quantify the sensitivity of one module to another in isolation from the network[3].

The MAPK network was systematically perturbed by downregulating protein levels using RNA interference (RNAi; Fig. 1c). To overcome possible functional redundancy, Erk1 and Erk2, Mek1 and Mek2 and Raf-1 and B-Raf isoenzymes were considered functional modules and simultaneously targeted by small interfering RNAs (siRNAs). For each perturbation, global response coefficients were derived (Fig. 1d) from quantitative western blots (see Supplementary Information, Fig. S1c), in which the phosphorylation status of Erk1/2, Mek1/2 and Raf-1 was measured. The monitored phosphorylation sites reflect the active state for each kinase[9–11]. To account for the steady-state assumption in MRA, the network responses were measured 15 min after NGF stimulation, where Erk phosphorylation is stable over time. For EGF stimulation, network responses were measured at the peak of Erk activity at 5 min (and 5 min NGF for comparison) where a (pseudo-)steady state can be assumed for a limited time span. The MAPK network topologies in PC-12 cells were determined by computing local response coefficients from the

[1]European Molecular Biology Laboratory (EMBL), Cell Biology and Biophysics, Meyerhofstrasse 1, D-69117 Heidelberg, Germany. [2]MPI for Molecular Physiology, Department of Systemic Biology, Otto-Hahn Strasse -11, 44227 Dortmund, Germany.
[3]Correspondence should be addressed to P.I.H.B. (e-mail: philippe.bastiaens@mpi-dortmund.mpg.de)

Received 29 November 2006; accepted 26 January 2007; published online 18 February 2007; DOI: 10.1038/ncb1543

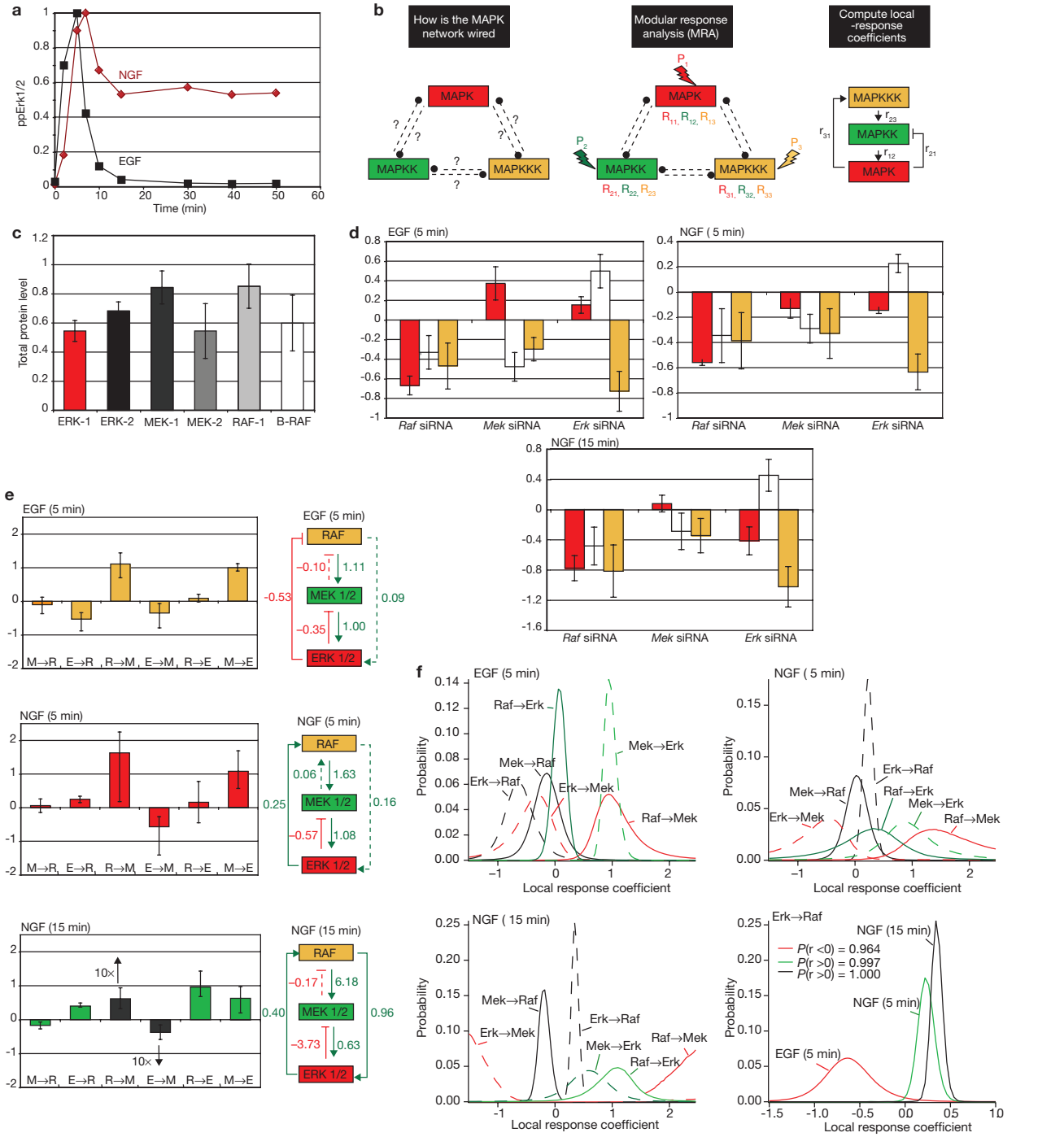

Figure 1 MRA reveals differences in MAPK-network topology. (**a**) Time-dependent Erk1/2 activity profile on stimulation with 100 ng ml^{-1} EGF and 50 ng ml^{-1} NGF derived from western blots. Normalized phosphorylated Erk1/2 (ppErk1/2) is shown on the *y* axis. (**b**) Schematic representation of MRA. Sensitivity analysis is performed on three functional modules: MAPK, MAPKK and MAPKKK for which sign and strength of connectivity are unknown. Systematic perturbations (P_j) are applied to each module (j) and the resulting change in activity of each module is determined as global response coefficient (R_{ij}). The connectivity from module j to module i, as if in isolation from the network, is obtained by computing local response coefficients (r_{ij})[3]. (**c**) Downregulation of total protein by double siRNAs (*Erk1* siRNA + *Erk2* siRNA, *Mek1* siRNA + *Mek2* siRNA and *Raf-1* siRNA + *B-Raf* siRNA) relative to unperturbed samples (mean ± s.d. of $n = 6$ data sets). (**d**) Average global response coefficients (GRC) for EGF and NGF (5 min) and NGF (15 min) stimulation (mean ± s.d. of $n = 4$ data sets for each perturbation). The perturbations are represented on the *x* axis (*Raf* siRNA, *Mek* siRNA and *Erk* siRNA). Average GRC are depicted for pRaf-1 (red), pMek1/2 (white) and pErk1/2 (orange). (**e**) Computed local response coefficients. Error bars represent estimated 68% confidence intervals computed from an over-determined system of four independent experimental sets for each condition: EGF (5 min), NGF 5 and 15 min. Connection pairs are given on the *x* axis. Grey bars in the NGF 15 min panel represent values scaled down by a factor of ten. R, M and E indicate Raf-1, Mek1/2 and Erk1/2, respectively. Corresponding MAPK network wiring diagrams are also shown. Dashed lines represent weak or no connectivity. (**f**) Error propagation in MRA estimated by Monte Carlo simulations. Probability distribution of LRCs for 5 min EGF stimulation, 5 min NGF stimulation and 15 min NGF stimulation. The bottom right panel contains the LRC probability distributions of the Erk–Raf feedback for EGF and NGF stimulation. Likelihoods (*P*) for sign of the LRCs for the Erk→Raf connection are given as determined from the probability distributions (see Supplementary Information, Fig. S1f).

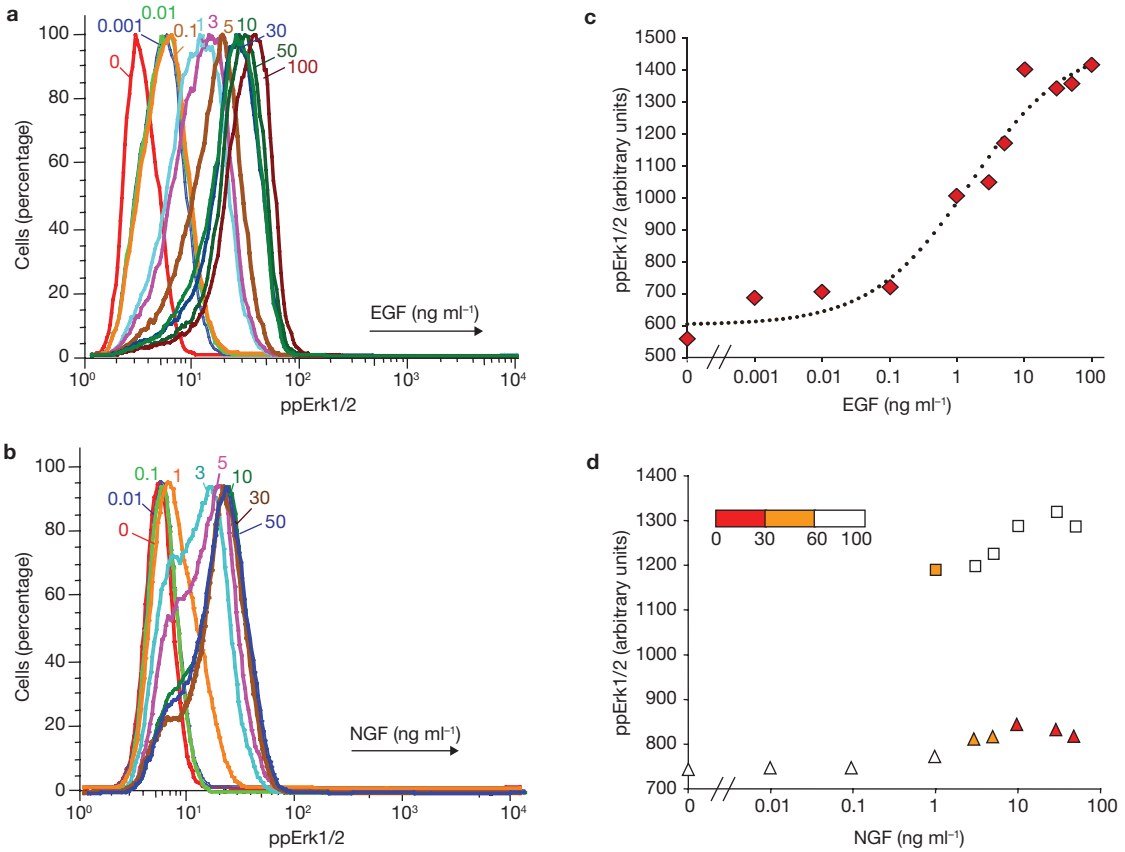

Figure 2 Dose-response profiles of Erk1/2 activation. (**a**, **b**) Flow cytometry histograms of ppErk1/2 response to increasing doses of EGF (**a**) and NGF (**b**). (**c**) Means of ppErk1/2 fluorescence intensity distribution are shown as function of EGF concentration. A sigmoid function was fitted to the experimental values (dotted line). (**d**) Means of ppErk1/2 fluorescence intensity (*y* axis) for each peak in the bimodal distribution are shown as a function of NGF concentration. Means of individual distributions were derived from fitting two Gaussian functions to the bimodal histograms (see Supplementary Information, Fig. S2). Triangle and squares represent the first and second peaks in the bimodal distribution, respectively. The colour bar represents the percentage of cells. The data shown is representative of $n = 3$ independent experiments, in which 10^5 cells were analysed each time.

over-determined system of four independent global response data sets for each experimental time point[12] (Fig. 1e and see Supplementary Information, Fig. S1d). The connections illustrated by the wiring diagrams represent either direct or indirect regulations[3]. We thus confirmed the positive regulatory connections from Raf-1 to Mek1/2 to Erk1/2, for both EGF and NGF stimulated cells. The observed negative feedback between Erk1/2 and Mek1/2 for both EGF and NGF activated networks has also been described in another cell system[13], where Erk directly phosphorylates Mek1. The regulatory influence from Raf-1 to Erk1/2 in the NGF-driven pathway may result from cross-cascade activation of Erk1/2 (ref. 14), or can be explained by the observation that B-Raf is the predominant MAPK kinase kinase (MAPKKK) in the NGF signalling network[7]. Most strikingly, MRA uncovered different feedback regulation from Erk1/2 to Raf-1 when the network was activated by the distinct growth factors — a negative feedback in the case of EGF stimulation and positive feedback for NGF stimulation. The analysis of NGF signalling over time demonstrated an increase in connectivity strength of this positive feedback. Moreover, if knowledge of the Raf–Mek–Erk hierarchy in the MAPK pathway is taken into account, this difference in regulatory feedbacks is also apparent from the global response coefficients. In the case of EGF stimulation, down-regulation of Erk1/2 gave a positive global response coefficient for RAF (increased activity), whereas for NGF stimulation this response coefficient was negative (decreased activity), suggesting negative and positive feedback, respectively (Fig. 1d). Furthermore, inhibition of Mek activity using PD184352 resulted in the loss of Raf-1-sustained activity after NGF stimulation (see Supplementary Information, Fig. S1e), confirming the existence of the NGF-driven positive feedback. Monte Carlo simulations were performed to estimate the probability distributions of the computed local response coefficients, and to determine intervals of confidence given the variance of the measured data (Fig. 1f and see Supplementary Information, Fig. S1f). The likelihood that the feedback from Erk to Raf is negative on EGF and positive on NGF stimulation was highly significant ($P = 0.96$ and $P = 1.00$, respectively).

From the growth-factor context-dependent MAPK topologies revealed by MRA, specific time and dose response properties of Erk1/2 activation can be predicted. The negative feedback observed on EGF stimulation explains the transient activation of Erk1/2, and was shown to be mediated by Erk1/2 downregulation of Son of Sevenless (SOS). In the case of MAPK network activation by NGF, MRA identified a positive feedback from Erk to Raf, which could sustain the prolonged Erk1/2 activity. The temporal activation profiles of Raf-1 and Mek1/2 (see Supplementary Information, Fig. S1b) reflect those of Erk1/2, showing that the elements within the MAPK core are encompassed by the feedback. The existence of a positive feedback endows the MAPK network with the potential for bistability, resulting in a switch-like NGF dose-response[16]. However, this property is dependent on feedback strength, which is determined by the

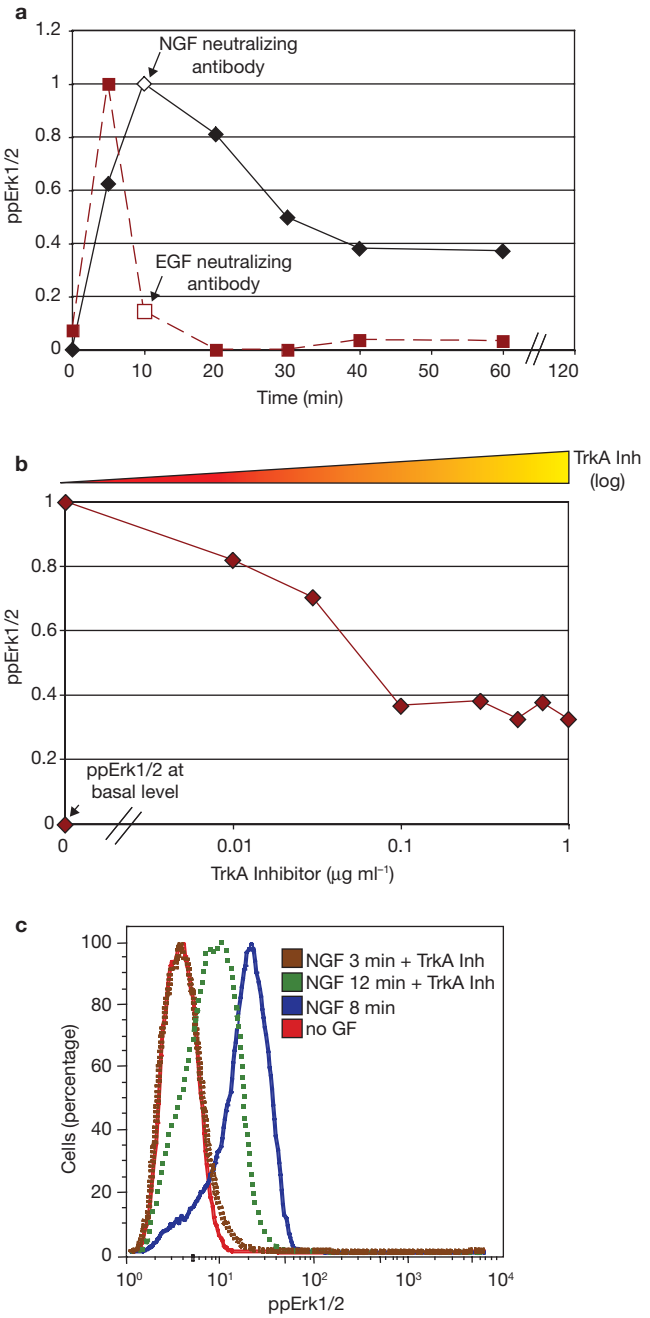

Figure 3 Irreversibility in MAPK network activation on NGF stimulation. (**a**) Phosphorylated Erk1/2 in response to EGF and NGF neutralizing antibodies. PC-12 cells were stimulated with EGF or NGF for 10 min followed by growth factor-neutralizing antibody treatment for the indicated times. (**b**) NGF induced ppErk1/2 in response to TrkA inhibition. Increasing doses of TrkA inhibitor (Inh; μg ml^{-1}) were added for 5 min to cells previously exposed to NGF for 12 min. (**c**) Flow cytometry histograms of ppErk1/2 stimulated with NGF at early (brown) and late (green) times followed by 5 min TrkA inhibition (12 μM). Untreated cells (no growth factor, GF; red) and NGF only treated cells (blue) were experimental controls. Approximately 10^5 cells were analysed for each condition.

kinetic properties of the involved enzymes — parameters difficult to determine experimentally[16,17]. Therefore, Erk1/2 responses to different EGF and NFG doses were measured directly by flow cytometry, and the distribution of Erk1/2 activation was analysed on a single-cell level (Fig. 2).

Although increasing EGF concentration resulted in a gradual increase in Erk1/2 phosphorylation, increasing NGF concentration resulted in a switch-like response, showing no intermediate states of Erk1/2 activation. The appearance of a bimodal distribution above a NGF threshold concentration clearly points to the existence of two discrete populations of phosphorylated Erk1/2. This bistability in the MAPK network could potentially promote a dynamically maintained memory of the NGF stimulus. As hysteresis, to the point of irreversibility, is a hallmark of bistability[18], we investigated how a decrease in stimulus after full Erk1/2 activation affected its phosphorylation. Whereas on EGF stimulation and treatment with EGF-neutralizing antibody Erk1/2 activity was virtually zero, the NGF inhibition profile showed 38% of Erk1/2 sustained activity (Fig. 3a and see Supplementary Information, Fig. S3a, b). To exclude the possibility that a fraction of internalized activated TrkA was still signalling to Erk1/2, the phosphorylated Erk1/2 profile in PC-12 cells treated with TrkA inhibitor was examined after NGF stimulation. Approximately 40% of active Erk1/2 was maintained (Fig. 3b, c) on full inactivation of TrkA (see Supplementary Information, Fig. S3c, d). When TrkA inhibitor was added before full Erk1/2 activation by NGF, the phosphorylation of Erk1/2 was not sustained (Fig. 3c). This indicates that the positive feedback confers bistability on the MAPK network after maximal activation of Erk1/2.

As the network topology underlies Erk dynamics, thereby governing specific cell fate, it should be possible to modulate MAPK dynamics and swap EGF- or NGF-induced PC-12 cell phenotype by interfering with the regulatory feedbacks. A MAPK positive-feedback mechanism from Erk to Raf involving protein kinase C (PKC) has been proposed[19]. PKC inhibition by Gö7874 resulted in transient Erk1/2 activation after NGF treatment, which is more characteristic for EGF stimulation (Fig. 4a and see Supplementary Information, Fig. S4a). Moreover, PKC inhibition specifically promoted proliferation (and not differentiation) of PC-12 cells on NGF stimulation (Fig. 4b). Control cells treated with Gö7874 alone, or NGF, showed S-phase entry similar to non-stimulated cells.

To achieve the complementary situation in which EGF stimulation results in cell differentiation, a positive feedback must be established in the MAPK module. As PKC inactivation resulted in the loss of the positive feedback on NGF stimulation, the expectation was that sustained activation of PKC by phorbol-12-myristate-13-acetate (PMA) would result in cell differentiation. This was not observed (Fig. 4d and see Supplementary Information, Fig. S4e), indicating that PKC activity is not part of the feedback loop, but functions upstream of the MAPK module to induce the positive feedback. In fact, we showed that the PKC activator, PLA2, did not function in the positive feedback (see Supplementary Information, Fig. S4b), as was proposed for other cell systems[19]. Furthermore, EGF stimulation in conjunction with PKC activation by PMA gave rise to a sustained Erk1/2 activation profile (Fig. 4c and see Supplementary Information, Fig. S4c). The amplitude and duration of Erk1/2 phosphorylation on PMA stimulation alone was 2.5-fold lower than the activation on NGF stimulation (see Supplementary Information, Fig. S4d). Importantly, the cells activated with EGF, in conjunction with PMA, differentiated as if stimulated by NGF (Fig. 4d and see Supplementary Information, Fig. S4e). Moreover, this was shown to be specifically dependent on PKCδ using RNAi experiments. On downregulation of PKCδ levels, the number of cells that differentiated was substantially lower than on NGF stimulation or on EGF stimulation in the presence of PMA (Fig. 4d and see Supplementary Information, Fig. S4e).

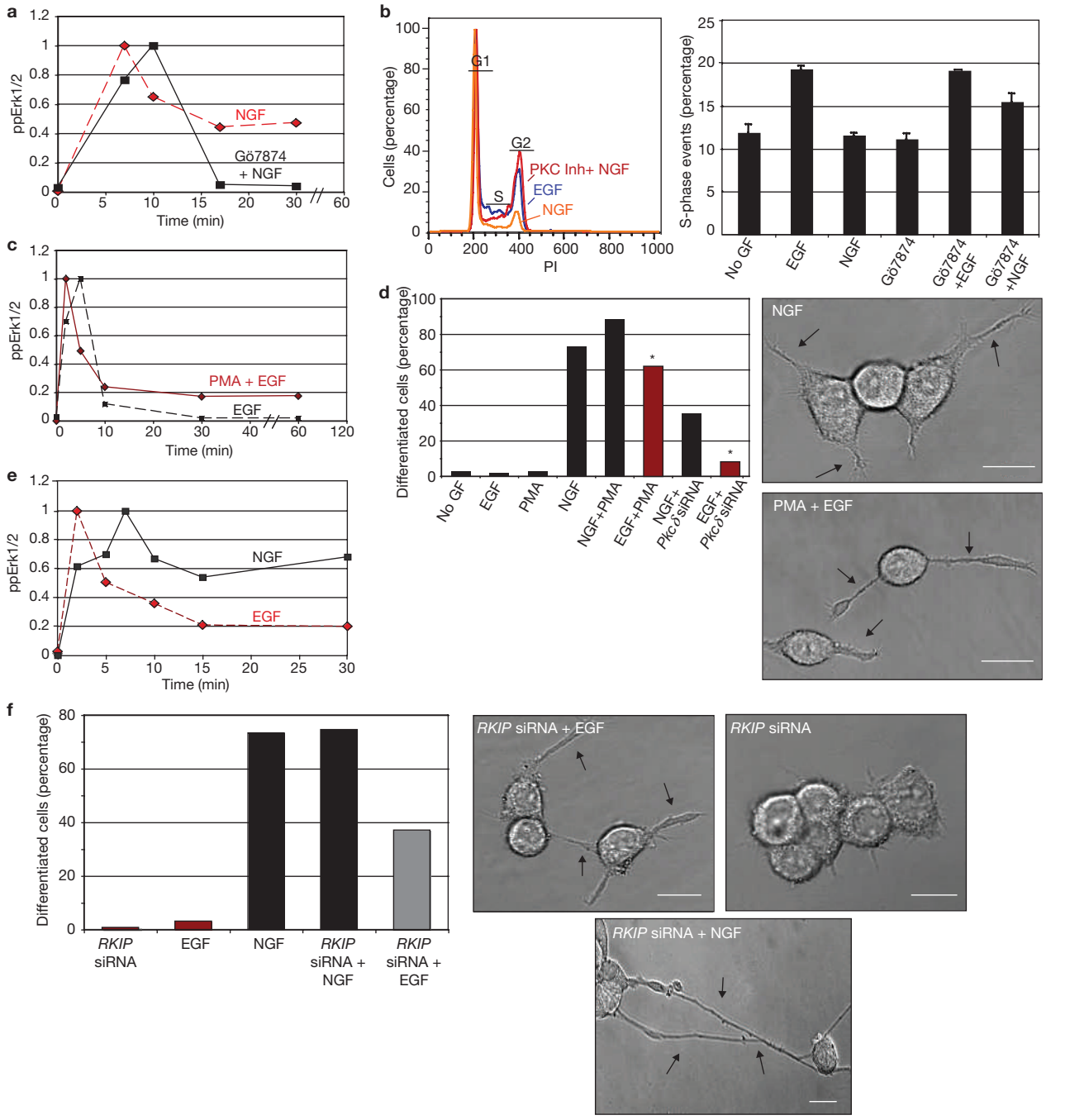

Figure 4 Rewiring MAPK-network topology redirects phenotypic response of PC-12 cells. (**a**) Time-dependent normalized Erk1/2 phosphorylation after NGF stimulation in the presence (solid line) or absence (dashed line) of PKC inhibitor Gö7874, analysed by western blot (see Supplementary Information, Fig. S4a). (**b**) Cell-cycle profiles of PC-12 cells stimulated with EGF, NGF and PKC inhibitor treatment followed by NGF. DNA content is represented by propidium iodide (PI) fluorescence intensity for 1×10^4 cells for each condition. The percentage of cells in S-phase for the indicated experimental conditions is also shown. The error bars represent mean ± s.d. of $n = 3$ data sets). (**c**) Time-dependent normalized ppErk1/2 response after EGF stimulation in the presence and absence of PMA, analysed by western blot (see Supplementary Information, Fig. S4c). (**d**) Neuronal differentiation of PC-12 cells on the indicated treatments analysed by DIC imaging. *PKCδ* siRNA-mediated downregulation of PKCδ isoform is indicated. The total number of cells analysed was 3,645. Representative DIC images of NGF stimulated and PMA followed by EGF stimulated PC-12 cells are shown. The arrows indicate neurite outgrowths. (**e**) Time-dependent profiles of ppErk1/2 after EGF and NGF stimulation in PC-12 cells where RKIP was downregulated to 60% by *RKIP* siRNA (see Supplementary Information, Fig. S4g). Asterisks indicate PMA- and EGF-treated cells. (**f**) Neuronal differentiation of PC-12 cells with the indicated treatments analysed by DIC imaging. The total number of cells analysed was 3,100. Representative DIC images of *RKIP* siRNA-treated non-stimulated cells, *RKIP* siRNA-treated NGF-stimulated cells and *RKIP* siRNA-treated EGF-stimulated cells. The arrows indicate neurite outgrowth. The scale bars represent 10 μm in **d** and **f**.

As these experiments suggest that PKC activity acts upstream of the MAPK module to induce the positive feedback, we investigated the effect of modulating a regulator of the MAPK network that is a substrate of PKC[20,21]. Raf kinase inhibitory protein (RKIP) is known for its negative role in MAPK signalling[22] by interfering with Raf-1 activation of Mek. Downregulation of RKIP by RNAi results in sustained Erk1/2 activation on EGF stimulation and increases the amplitude of sustained NGF-driven activity (Fig. 4e and see Supplementary Information, Fig. S4f, g). Under these conditions, PC-12 cell differentiation occurred in cells stimulated with EGF (Fig. 4f). These results indicate a role for RKIP in negatively regulating the positive feedback. In a recent study[23], the carboxyl terminus of Raf-1 was shown to be phosphorylated *in vivo* by Erk1/2 in a growth factor-dependent manner. The authors proposed a positive feedback from Erk1/2 to Raf-1, which not only enhances the kinase activity of Raf-1, but also promotes its sustained activity. Another report[21] demonstrated that PKC phosphorylation of RKIP promoted Erk1/2 activation by decreasing the affinity of RKIP for Raf-1. It is, therefore, conceivable that the positive feedback observed in NGF signalling is driven by a synergistic mechanism through which PKC-mediated phosphorylation of RKIP removes this protein from Raf-1, thereby enabling direct Raf-1 phosphorylation by Erk1/2.

We have demonstrated that Erk1/2 activation dynamics are critically determined by the manner in which the MAPK network is wired. By interfering with these topological features, and thereby Erk activation dynamics, we were able to redirect the specific growth factor-induced cell fates. We propose, therefore, that EGF or NGF stimulation induces a specific molecular context characterized by the activation of a distinct set of positive and negative regulators of the MAPK network, such as PKC. These regulators are differentially activated by EGFR and TrkA, and therefore possess different activation kinetics and sub-cellular localization. The distinct molecular contexts modulate the connectivity between components of the MAPK network, giving rise to a growth factor-specific network topology. Our results highlight the importance of studying network topologies in signal transduction to understand complex dynamics. MRA, as applied here, can be used to study larger networks to uncover network motifs that generate particular dynamics of signalling molecules that control cell fate. □

METHODS

Antibodies and inhibitors, Anti-Erk1/2, anti-phosphoErk1/2, anti-phospho-Mek1/2, anti-phospho-TrkA, anti-pEGFR (Y845), anti-pMarcks (S152/156), anti-RKIP and anti-Raf-1 (S296) were purchased from Cell Signaling Technology (Beverly, MA). Anti-phospho-Raf-1 (Ser 338) and anti-TrkA were purchased from Upstate (Chandlers Ford, UK). α-Tubulin mouse antibody was from Sigma-Aldrich (Munich, Germany). pS62 antibody (for a nuclear pore protein) was a gift from I. Mattaj (EMBL, Heidelberg, Germany). Secondary staining for quantitative western blots was performed with goat anti-mouse, rabbit or rat IRDye 800CW from Rockland Immunologicals (Gilbertsville, PA) and goat anti-mouse, rabbit or rat Alexa-680 from Molecular Probes (Karlsruhe, Germany). Kinase inhibitors used were Gö7874, hydrochloride, TrkA inhibitor, wortmannin, MAFP and PMA, all from Calbiochem. PD184352 was a generous gift from P. Cohen (MRC, Dundee University, UK). Blocking peptide for EGF and NGF were from R&D Systems (Minneapolis, MN) and Biomedical Technologies (Stoughton, MA), respectively.

Cell line. PC-12 cells from ATTC (Wesel, Germany) were cultured in collagen-coated(100 μg) dishes at 37 °C, 5% CO_2 in DMEM supplemented with 10% donor horse serum, 5% FCS, glutamine and antibiotics. For starvation conditions, cells were maintained overnight in DMEM supplemented with 1% horse serum, glutamine and antibiotics.

siRNA knockdowns. Perturbations of MAPK network were performed by using siRNA rat specific SMARTpools against *Erk1*, *Erk2*, *Mek1*, *Mek2*, *Raf-1*, *BRaf*, *RKIP* (human) and PKCδ, all purchased from Dharmacon Research (Bonn, Germany). For every experiment performed, siRNA non-targeting, RNA-induced silencing complex (RISC)-free and mock transfection were used as controls. Transfection of siRNAs into PC-12 cells was done for 24 h with Dharmafect2 from Dharmacon Research according to the manufacturer's recommendations. Levels of knockdown were tested after 72 h by examining protein levels using total antibodies.

Modular response analysis. Perturbations of the MAPK network were performed by RNAi using siRNAs as described above. PC-12 cells transfected with siRNAs and control cells (nontargeting siRNA, RISC-free and mock transfection) were stimulated with EGF or NGF for 5 or 15 min. Activities of Raf-1, Mek1/2 and Erk1/2 were detected simultaneously by using phospho-specific antibodies. Levels of downregulation and activities were normalized using antibodies for total protein. MRA was implemented to derive the local response matrix (r_{ij}), which quantifies the sensitivity of component i to component j in the network. Briefly, the change in the steady state concentration (x_i) of each component in the network in response to a perturbation (P_j) is given by the global response matrix $R_{ij} = \partial \ln x_i / \partial \ln p_j$, which was estimated by the formula $Rij \approx 2(x_i^{(1)} - x_i^{(0)})/(x_i^{(1)} + x_i^{(0)})$, where $x_i^{(0)}$ and $x_i^{(1)}$ are the steady-state concentrations of component x_j before and after perturbation, respectively. The local response matrix r_{ij}, was calculated from R_{ij} using a program written in Python (http://www.python.org), by solving $\sum_k r_{ik} R_{kj} = 0$, using total least squares estimation as previously described[12]. The errors were evaluated by estimating the probability distributions of the response coefficients r_{ij} given the measured steady-state concentrations x_i using Monte Carlo simulations. In the simulations, random realizations of the steady-state concentration y_i were drawn from a normal distribution with mean and standard deviation equal to those of the measured value x_i. Response matrices r_{ij} were calculated for 1×10^6 realizations of y_i, and histograms of the resulting local response coefficients were calculated and plotted using Igor Pro (WaveMetrics, Lake Oswego, OR). The probability that a response coefficient r_{ij} was larger (or smaller) than zero was estimated by the fraction of realizations that was larger (or smaller) than zero. In addition, 68% confidence intervals, which correspond to one standard deviation of a normal distribution, were calculated from the estimated probability functions. The lower bound of the confidence interval was estimated by the value below which 16% of the realizations were found. The upper bound was estimated by the value below which 84% of the realizations were found. MRA-uncovered network wiring describes both direct and indirect regulatory connections, the latter allowing for regulations through unknown components of the network to be depicted.

Quantitative western blot assays. Cell lysates separated by SDS–PAGE (see Supplementary Information, Methods) were transferred to PDVF membranes. Secondary antibodies labelled with Alexa 680 and IRDye 800 were used for visualization. Detection and quantification was performed with the Odyssey Infrared Imaging System (LI-Cor Biosystems, Homburg, Germany). Scanning of membranes was performed at 700 nm and 800 nm simultaneously with an Odyssey instrument at 169 μm resolution, medium quality, focus offset 3.0 mm and intensity setting of five for the 700 nm channel and of three for 800 nm channel. Normalization of gel bands was accomplished by ratiometric analysis of two wavelengths, where α-tubulin or total protein was used as loading control.

Flow cytometry. FACS experiments were performed as previously described[24]. Briefly, cells were fixed with 1.5% PFA and permeabilized by adding 90% ice-cold methanol. Primary staining was performed with monoclonal phospho-Erk1/2 antibody labelled with Alexa647 (BD Biosciences, Heidelberg, Germany). The measurements were performed on a MoFlo cytometer (DakoCytomation, Glostrup, Denmark) and data acquired with summit V3.1 Buil 839 software. Cell-cycle experiments were done in FACScan flow cytometer (BD Biosciences Immunocytometry Systems, Erembodegem, Belgium) equipped with an argon ion laser. Cell preparation for cell-cycle analysis was performed by starving cells for 24 h and treatment of cells with growth factors or/and inhibitors for a further 16 h. Cells were fixed with 70% ethanol and stained with propidium iodide solution (0.1% (v/v) Triton X-100 in PBS, 2 mg DNase free RNase A (Sigma) and 1 mg ml^{-1} propidium iodide (Molecular Probes) for 20 min before analysis in

FACScan cytometer. FlowJo software 6.2.1 was used for quantification and analysis of all data. For every flow cytometry analysis, FSC and SSC (forward and side scatter, respectively) gating was performed, to exclude doublets and debris.

Differential interference contrast (DIC) microscopy. PC-12 cells were grown in poly-L-lysine coated μ-Dishes (Ibidi, Munich, Germany) in starving conditions for 12 h. Cells were either left untreated or were treated with EGF, NGF, PMA (200 nM) or *RKIP* siRNA. DIC microscopy was performed 48 h after treatments in a Leica AOBS SP2 system equipped with a 63× 1.4 NA oil immersion objective. Quantification was done by dividing the number of differentiated cells by the total cell number from 10 different images for each experimental condition. A total number of 3100 cells were analysed. The criteria for defining differentiated cells were cell flattening and neurite outgrowth at least as long as the cell body.

Note: Supplementary Information is available on the Nature Cell Biology website.

ACKNOWLEDGEMENTS

We are thankful to G. Nolan for FACS protocols and to A. Riddell (Flow Cytometry Core Facility, EMBL) for technical assistance. We also thank P. Cohen, A. Squire, P. Beltrao and A. Kinkhabwala for very helpful discussions. S. Santos is supported by an 'E-STAR' fellowship funded by the ECs FP6 Marie Curie Host fellowship for Early Stage Research Training under contract number MEST-CT-2004-504640.

COMPETING FINANCIAL INTERESTS

The authors declare that they have no competing financial interests.

Published online at http://www.nature.com/naturecellbiology/
Reprints and permissions information is available online at http://npg.nature.com/reprintsandpermissions/

1. O'Neill, E. & Kolch, W. Conferring specificity on the ubiquitous Raf/MEK signalling pathway. *Br. J. Cancer* **90,** 283–288 (2004).
2. Greene, L. A. & Tischler, A. S. Establishment of a noradrenergic clonal line of rat adrenal pheochromocytoma cells which respond to nerve growth factor. *Proc. Natl Acad. Sci. USA* **73,** 2424–2428 (1976).
3. Kholodenko, B. N. *et al.* Untangling the wires: a strategy to trace functional interactions in signaling and gene networks. *Proc. Natl Acad. Sci. USA* **99,** 12841–12846 (2002).
4. Marshall, C. J. Specificity of receptor tyrosine kinase signaling: transient versus sustained extracellular signal-regulated kinase activation. *Cell* **80,** 179–185 (1995).
5. Murphy, L. O., Smith, S., Chen, R. H., Fingar, D. C. & Blenis, J. Molecular interpretation of ERK signal duration by immediate early gene products. *Nature Cell Biol.* **4,** 556–564 (2002).
6. Schoeberl, B., Eichler-Jonsson, C., Gilles, E. D. & Muller, G. Computational modeling of the dynamics of the MAP kinase cascade activated by surface and internalized EGF receptors. *Nature Biotechnol.* **20,** 370–375 (2002).
7. Kao, S., Jaiswal, R. K., Kolch, W. & Landreth, G. E. Identification of the mechanisms regulating the differential activation of the mapk cascade by epidermal growth factor and nerve growth factor in PC12 cells. *J. Biol. Chem.* **276,** 18169–18177 (2001).
8. Sasagawa, S., Ozaki, Y., Fujita, K. & Kuroda, S. Prediction and validation of the distinct dynamics of transient and sustained ERK activation. *Nature Cell Biol.* **7,** 365–373 (2005).
9. Diaz, B. *et al.* Phosphorylation of Raf-1 serine 338-serine 339 is an essential regulatory event for Ras-dependent activation and biological signaling. *Mol. Cell Biol.* **17,** 4509–4516 (1997).
10. Anderson, N. G., Maller, J. L., Tonks, N. K. & Sturgill, T. W. Requirement for integration of signals from two distinct phosphorylation pathways for activation of MAP kinase. *Nature* **343,** 651–653 (1990).
11. Alessi, D. R. *et al.* Identification of the sites in MAP kinase kinase-1 phosphorylated by p74raf-1. *EMBO J.* **13,** 1610–1619 (1994).
12. Andrec, M., Kholodenko, B. N., Levy, R. M. & Sontag, E. Inference of signaling and gene regulatory networks by steady-state perturbation experiments: structure and accuracy. *J. Theor. Biol.* **232,** 427–441 (2005).
13. Eblen, S. T. *et al.* Mitogen-activated protein kinase feedback phosphorylation regulates MEK1 complex formation and activation during cellular adhesion. *Mol. Cell Biol.* **24,** 2308–2317 (2004).
14. Frost, J. A. *et al.* Cross-cascade activation of ERKs and ternary complex factors by Rho family proteins. *EMBO J.* **16,** 6426–6438 (1997).
15. Buday, L., Warne, P. H. & Downward, J. Downregulation of the Ras activation pathway by MAP kinase phosphorylation of Sos. *Oncogene* **11,** 1327–1331 (1995).
16. Ferrell, J. E., Jr. & Machleder, E. M. The biochemical basis of an all-or-none cell fate switch in *Xenopus* oocytes. *Science* **280,** 895–898 (1998).
17. Ferrell, J. E., Jr. Building a cellular switch: more lessons from a good egg. *Bioessays* **21,** 866–870 (1999).
18. Kholodenko, B. N. Cell-signalling dynamics in time and space. *Nature Rev. Mol. Cell. Biol.* **7,** 165–176 (2006).
19. Bhalla, U. S., Ram, P. T. & Iyengar, R. MAP kinase phosphatase as a locus of flexibility in a mitogen-activated protein kinase signaling network. *Science* **297,** 1018–1023 (2002).
20. Corbit, K. C. *et al.* Activation of Raf-1 signaling by protein kinase C through a mechanism involving Raf kinase inhibitory protein. *J. Biol. Chem.* **278,** 13061–13068 (2003).
21. Lorenz, K., Lohse, M. J. & Quitterer, U. Protein kinase C switches the Raf kinase inhibitor from Raf-1 to GRK-2. *Nature* **426,** 574–579 (2003).
22. Yeung, K. *et al.* Suppression of Raf-1 kinase activity and MAP kinase signalling by RKIP. *Nature* **401,** 173–177 (1999).
23. Balan, V. *et al.* Identification of novel *in vivo* Raf-1 phosphorylation sites mediating positive feedback Raf-1 regulation by extracellular signal-regulated kinase. *Mol. Biol. Cell* **17,** 1141–1153 (2006).
24. Krutzik, P. O. & Nolan, G. P. Intracellular phospho-protein staining techniques for flow cytometry: monitoring single cell signaling events. *Cytometry* **55,** 61–70 (2003).

Figure S1

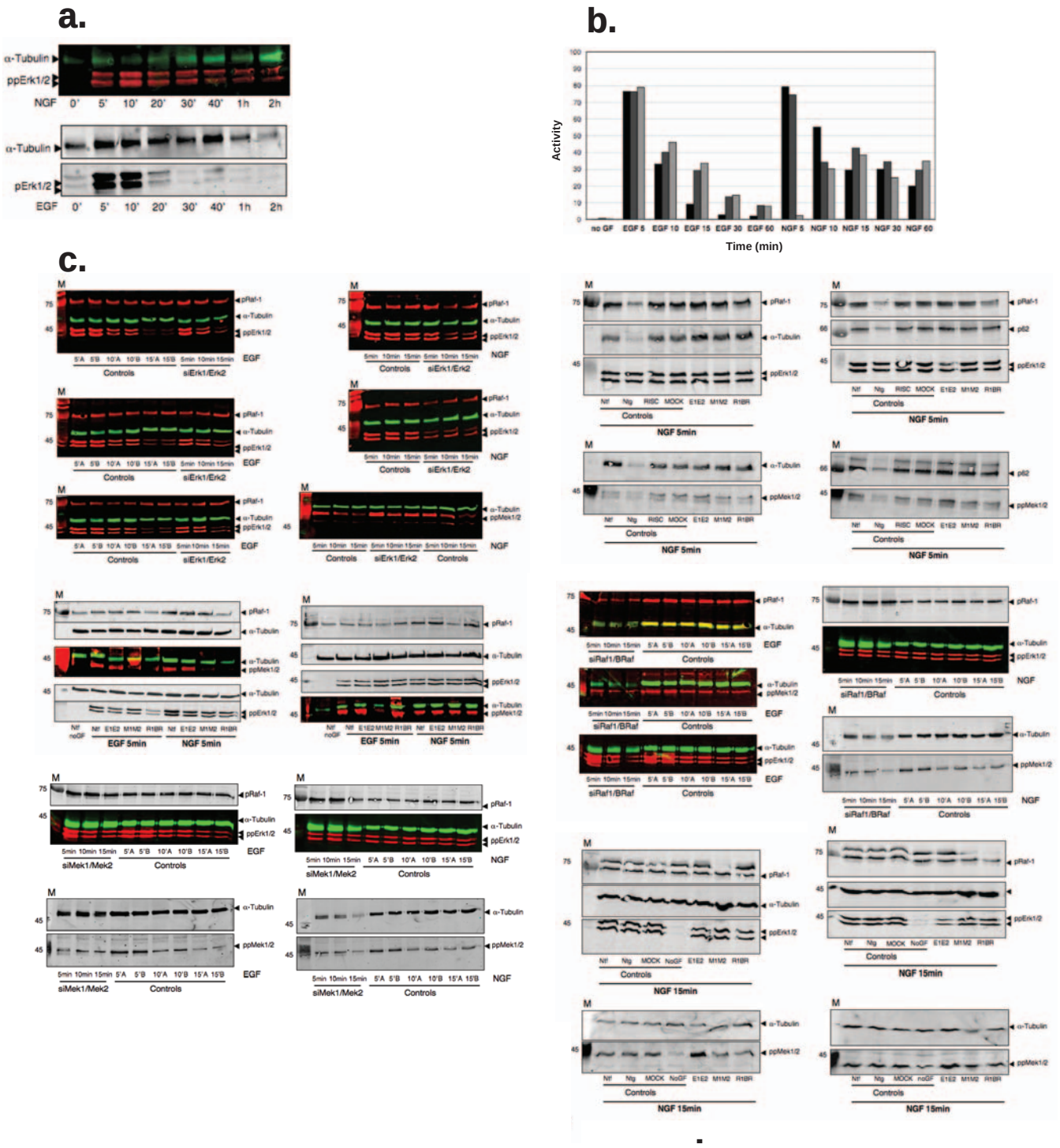

Figure S1. CONT.

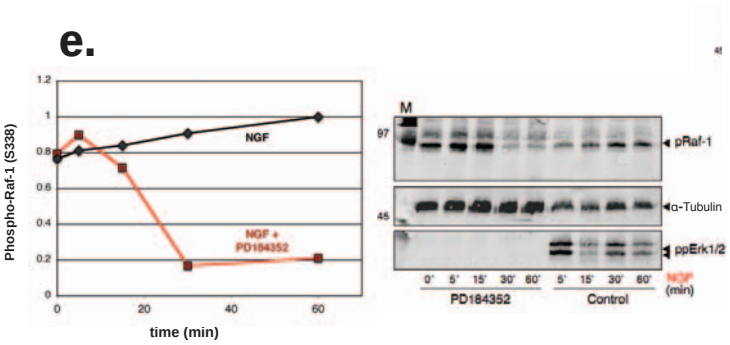

f.

EGF 5 minutes			
	68% Confidence interval		P > 0
	Lower bound	Upper bound	
Mek → Raf	- 0.37	+0.12	0.296
Erk → Raf	- 0.88	-0.32	0.036
Raf → Mek	0.78	1.52	0.996
Erk → Mek	-0.79	-0.07	0.106
Raf → Erk	-0.02	0.21	0.788
Mek → Erk	0.88	1.10	1.000
NGF 5 minutes			
	68% Confidence interval		P > 0
	Lower bound	Upper bound	
Mek → Raf	-0.14	0.26	0.611
Erk → Raf	0.16	0.35	0.997
Raf → Mek	1.01	3.02	0.963
Erk → Mek	-1.41	-0.17	0.088
Raf → Erk	- 0.45	0.88	0.679
Mek → Erk	0.47	1.59	0.936
NGF 15 minutes			
	68% Confidence interval		P > 0
	Lower bound	Upper bound	
Mek → Raf	-0.27	-0.07	0.057
Erk → Raf	0.31	0.43	1.000
Raf → Mek	2.97	9.11	0.999
Erk → Mek	-5.85	-1.59	0.044
Raf → Erk	0.69	1.43	0.975
Mek → Erk	0.20	0.98	0.911

Table 2: 68% Confidence intervals for the local response coefficients, derived from their probability density functions that were estimated by Monte Carlo simulations (see Methods)

d.

	EGF 5 minutes		
	Raf	Mek	Erk
siRNA Raf	-0.68619036	-0.86058334	-1.20113717
siRNA Mek	-0.12842569	-0.87060372	-0.95215206
siRNA Erk	-0.31103388	1.05525896	-0.71368895
siRNA Raf	-1.19055649	-0.29297206	-1.59356725
siRNA Mek	0.27231917	0.22774869	-0.1881955
siRNA Erk	-0.96319499	0.22435186	-1.66223414
siRNA Raf	-0.39531907	-0.91250734	-0.28093267
siRNA Mek	-0.09767814	-0.46534489	-0.36504135
siRNA Erk	-0.2286492	0.11023622	-1.24102056
siRNA Raf	-0.8325981	0.13465347	-0.18431002
siRNA Mek	0.26876685	-0.04812966	0.12513944
siRNA Erk	-0.15890993	0.41577801	-0.46901709
NGF 5 minutes			
	Raf	Mek	Erk
siRNA Raf	-0.60721868	-0.87840609	-0.99407429
siRNA Mek	-0.27618165	-0.47643055	-0.8503027
siRNA Erk	-0.10815451	0.18410351	-0.90832514
siRNA Raf	-0.5260274	0.08170213	0.06569804
siRNA Mek	0.06505771	-0.43478261	0.06569804
siRNA Erk	-0.1146789	0.43036212	-0.46835953
siRNA Raf	-0.59027266	-0.48844585	-0.38129029
siRNA Mek	-0.22257351	-0.27600497	-0.38350765
siRNA Erk	-0.21738582	0.19934426	-0.32152198
siRNA Raf	-0.51637174	-0.09862385	-0.2380005
siRNA Mek	-0.09171975	0.0237581	-0.149785
siRNA Erk	-0.14629509	0.0867747	-0.8399211
NGF 15 minutes			
	Raf	Mek	Erk
siRNA Raf	-0.50588235	-0.74226422	-1.15392388
siRNA Mek	0.07239819	-0.55260435	-0.0539592
siRNA Erk	-0.03098927	0.23093474	-0.77781074
siRNA Raf	-0.50107066	0.09848485	-0.39281576
siRNA Mek	0.08837971	-0.86039886	-0.62472196
siRNA Erk	0.23564955	0.22363765	-0.82296651
siRNA Raf	-0.83485873	-0.34045689	-0.16603853
siRNA Mek	0.66501487	-0.24947735	-0.25768709
siRNA Erk	0.34388366	0.59179713	-0.16703809
siRNA Raf	-0.83485873	-0.34045689	-0.16637872
siRNA Mek	0.66501487	-0.24947735	-0.25768709
siRNA Erk	0.06159032	0.94167117	-1.140721

Table 1: Matrices of global response coefficients used for calculating the local response coefficients

S1. (a) Western blots of active Erk1/2 (ppErk1/2) time series upon NGF (upper panel) and EGF (lower panel) stimulation. α -Tubulin was used as loading control for quantification. **(b)** Time profiles of activated Erk1/2 (black), Mek1/2 (dark grey) and Raf-1 (light grey) upon EGF and NGF stimulation measured simultaneously by polychromatic flow cytometry. **(c)** Western blots of primary data sets used for MRA for EGF and NGF 5 min and for NGF 15 min upon siErk1+siErk2, siMek1+siMek2 or siRaf-1+siB-Raf perturbations. α-Tubulin or p62 were used as loading control for quantification. **(d)** Mek inhibitor PD184352 attenuates MAPKKK activation upon NGF stimulation. Time series profiles of Raf-1 phosphorylation upon NGF stimulation with (■) and without (♦) Mek specific inhibitor PD184352. α-Tubulin was used as loading control for quantification.

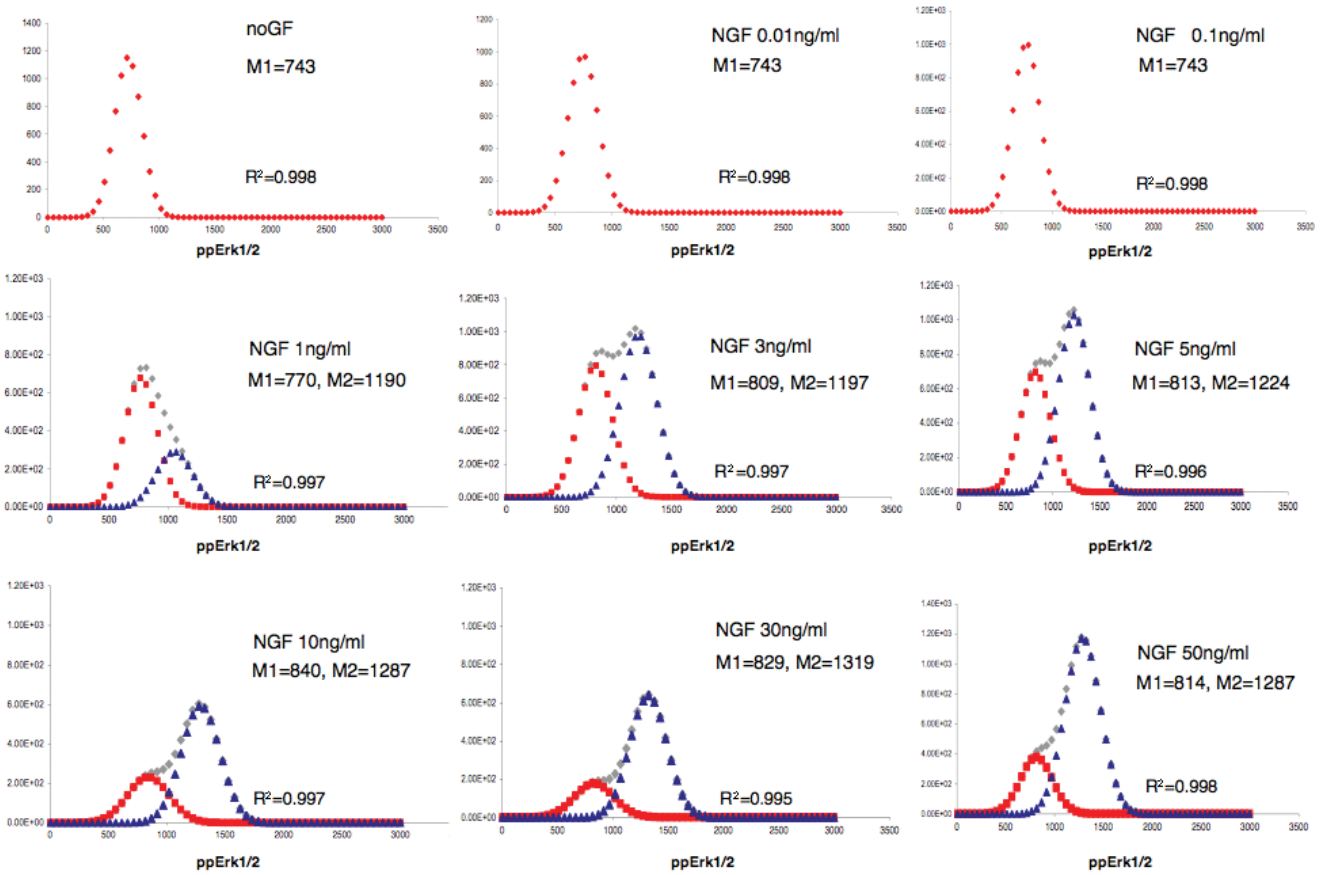

S2. Fitting two Gaussian functions to the bimodal ppErk1/2 population of NGF dose response histograms. The means of the fitted Gaussian functions are represented as M1 and M2. M1, in red, shows lower mean values of first ppErk1/2 population and M2, in blue, represent the second population. The experimental histograms are shown in grey. Data fitting was performed in Origin software.

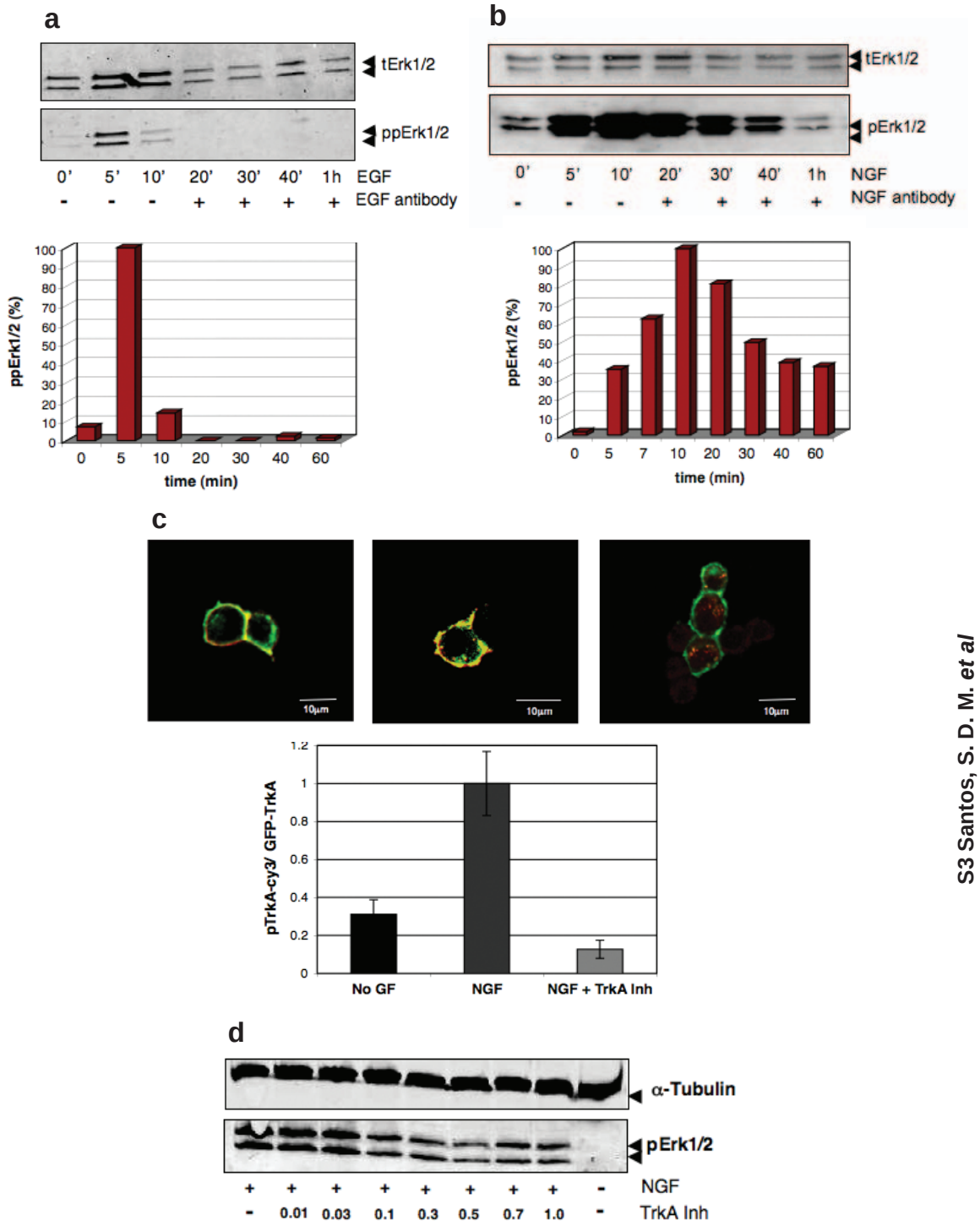

S3 Santos, S. D. M. *et al*

S3. (a) Western blot analysis of ppErk1/2 upon EGF stimulation after EGF neutralizing antibody treatment. Total Erk1/2 (tErk1/2) antibody was used as loading control. Bottom panel shows normalized quantification of Erk1/2 phosphorylation. **(b)** Western blot analysis of ppErk1/2 upon NGF stimulation after NGF neutralizing antibody treatment. Total Erk1/2 (tErk1/2) antibody was used as loading control. Lower panel shows normalized quantification of Erk1/2 phosphorylation **(c)** LSM confocal images of PC-12 cells ectopically expressing GFP-TrkA (green) and stained with anti-phospho-TrkA-cy3 antibody (red). Cells were either kept untreated (left), stimulated with NGF (50 ng/ml) for 12 min (middle) and NGF for 12 min followed by treatment with TrkA inhibitor at 12 µM for 5 min (right). Lower panel: quantification of fluorescence intensity as described in Supplementary Methods. (**d)** Western blot analysis of ppErk1/2 response to TrkA inhibition. Cells were stimulated with NGF 50 ng/ml for 12 min and TrkA inhibitor was added as indicated. Concentrations are shown in mg/ml. α-Tubulin was used as loading control for quantification.

S4

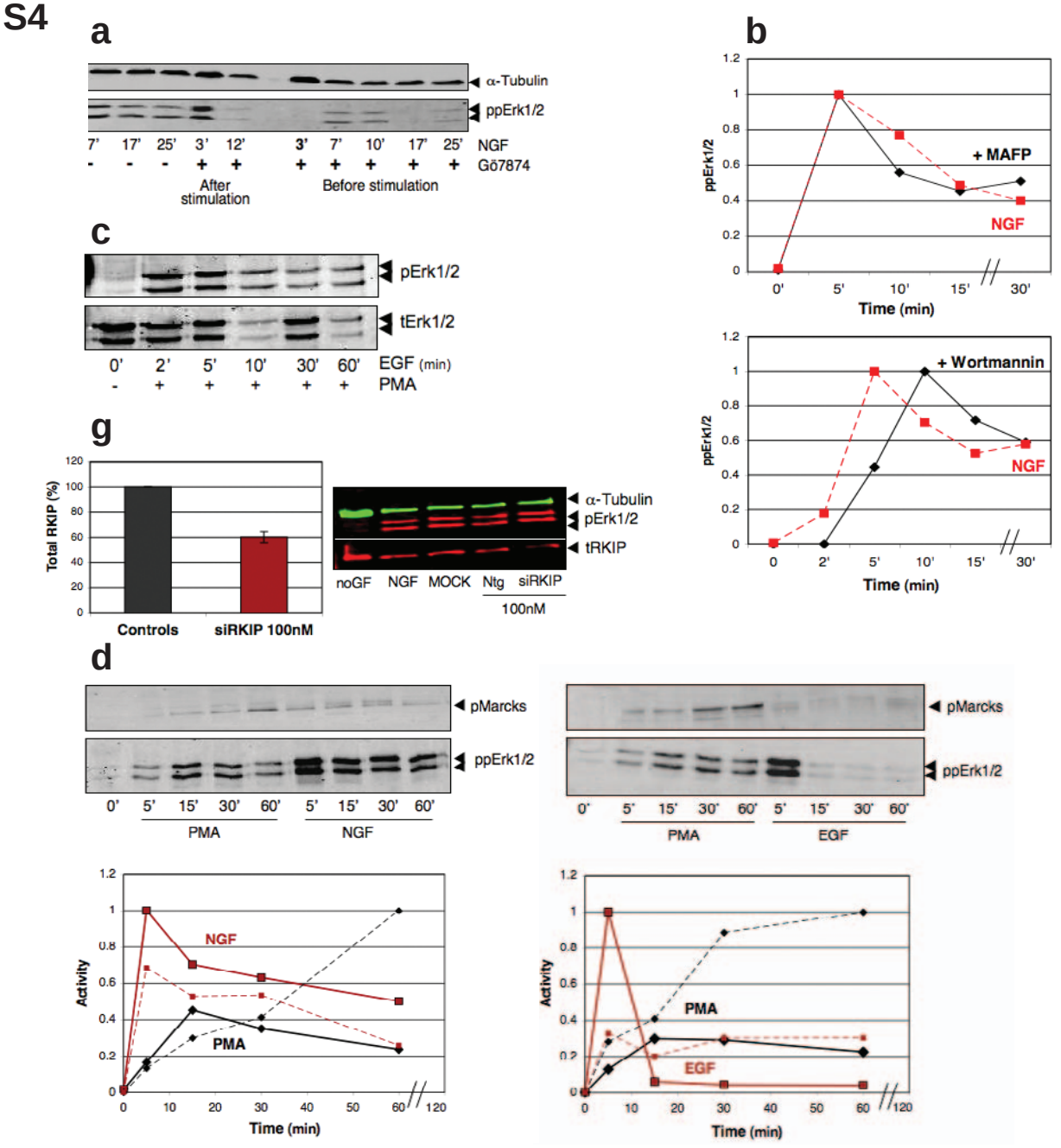

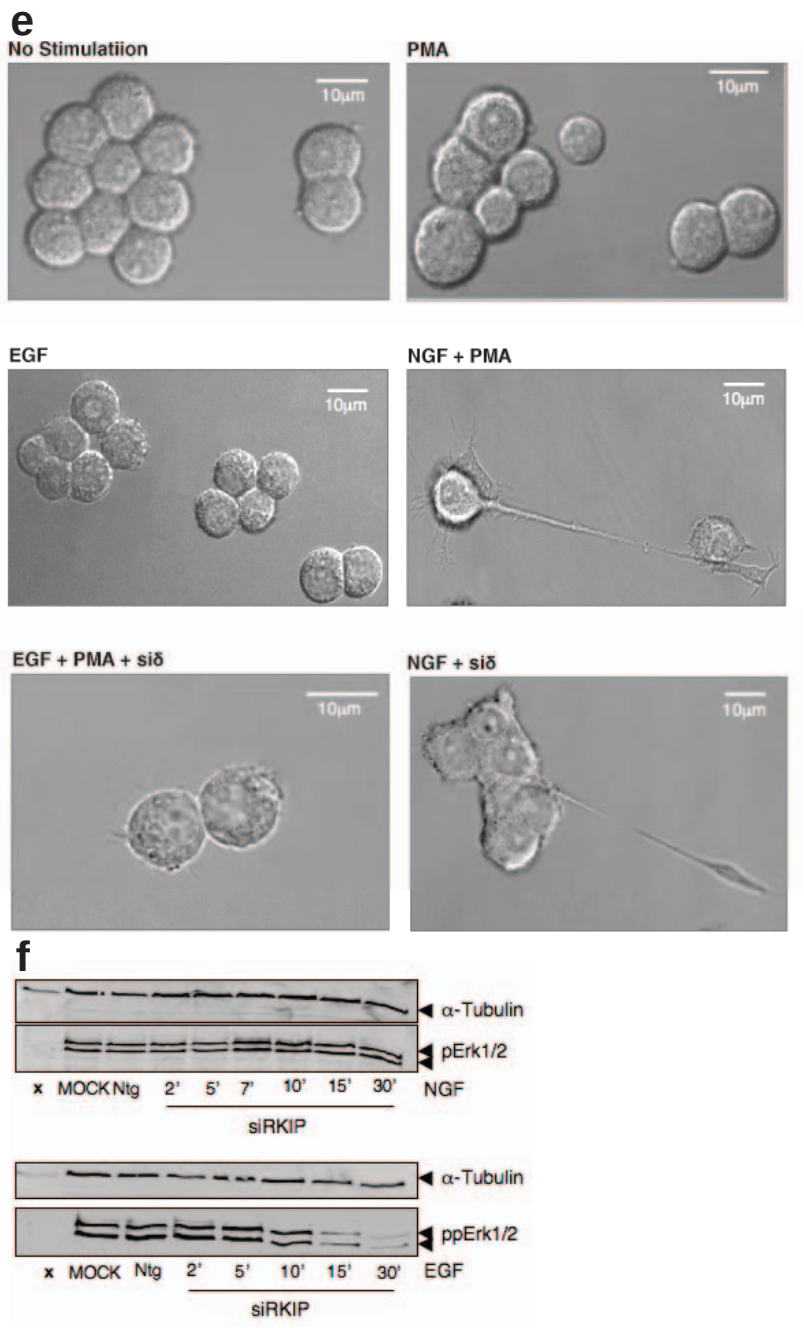

S4. (a) Western blot analysis of ppErk1/2 upon NGF stimulation and treatment with PKC inhibitor Gö7874 at 10 μM for 5 min. α-Tubulin was used as loading control for quantification. **(b)** PLA2 and PI3K inhibition does not interfere with ppErk1/2 sustained activation upon NGF stimulation. Upper panel: ppErk1/2 response to PLA2 inhibition (black solid line) by MAFP treatment (20 μM for 30 min) ppErk1/2 in response to NGF stimulation is shown as control (red dashed line). Lower panel: ppErk1/2 response to PIK3 inhibition by wortmannin at 100 nM for 30 min. ppErk1/2 response to NGF stimulation is shown in the absence (dashed line) and presence (solid line) of wortmannin. α-tubulin was used as loading control **(c)** Western blot analysis of ppErk1/2 upon EGF stimulation and simultaneous treatment with PKC activator (PMA) at 100 nM. Total Erk1/2 was used as loading control for quantification. **(d)** Western blot analysis of ppErk1/2 and pMarcks (PKC substrate) upon PMA and EGF treatment (left panel) and PMA and NGF treatment (right panel). Lower panels: quantification of phosphorylation levels. **(e)** Representative DIC images of experimental controls for PKC activation experiment. Untreated (top left), PMA (top right), EGF (middle left), NGF with PMA (middle right), EGF with PMA and PKCδ siRNA (bottom left) and NGF with PKCδ siRNA (bottom right) treated PC-12 cells are shown. **(f)** Western blot analysis of ppErk1/2 response upon NGF or EGF stimulation of siRKIP (100 nM) transfected PC-12 cells. Experimental controls: untreated (noGF), no siRNA transfection (MOCK) and non-targeting siRNA (Ntg). α-Tubulin was used as loading control. **(g)** Quantification of RKIP down-regulation by RNA interference. Western blot shows untreated (noGF), NGF 5 min stimulation (NGF), MOCK transfection (MOCK) and non-targeting siRNA (Ntg). α-Tubulin was used as loading control. Left panel: quantification of RKIP levels in control versus siRKIP treated cells.